JMEPEG (2011) 20:1414–1418
DOI: 10.1007/s11665-010-9777-z

1059-9495/$19.00

# Development of Precipitation Strengthened Steel with Adequate Stretch Flangeability

*B. Sarkar and B.K. Jha*

*(Submitted January 19, 2010; in revised form August 31, 2010)*

**An experimental steel of the composition (in wt.%) 0.04C-0.81Mn-0.38Si-0.15Ti-0.01S-0.013P-0.043Al was hot rolled into 4 mm plates at three different temperatures of 1100, 1000, and 900 °C. The yield strengths of these plates were in the range of 434-484 MPa while the ultimate tensile strength varied from 508 to 586 MPa. Elongation values ranged from 13.0 to 17.8%. Hole expansion ratios (λ) varied from 23 to 30.7%. In particular, the plate rolled at 1000 °C showed a yield strength of 484 MPa, an ultimate tensile strength of 586 MPa, a total elongation of ~15%, and a hole expansion ratio of ~23%. Transmission electron microscopy showed the presence of fine precipitates of titanium carbosulfide (~10-50 nm). Therefore, maximum precipitation strengthening was obtained in the plate that was hot rolled into a thickness of 4 mm at 1000 °C.**

**Keywords** ferrite, precipitation strengthening, stretch flangeability, TiC precipitation

## 1. Introduction

Development of high-strength, hot-rolled steel sheets forms part of the broad initiative for the weight reduction in automobiles. These steels are used to make suspension parts in automobiles. One of the requirements in the application of these steels is the so-called edge formability or stretch flangeability. This property is required for carrying out the flanging operation to create mating surfaces for the fabrication of the underbody parts in an automobile. For the steel sheets to have high stretch flangeability, it is desirable that the microstructure should be homogeneous. Hence, a single phase microstructure, for example, ferrite is suitable for this kind of application. Since ferrite is a soft phase, strengthening is achieved through the precipitates of titanium carbide. Titanium carbides have very high thermal stability. The free energy of formation of TiC is $-180$ kJ kg$^{-1}$ K$^{-1}$ compared to +6 kJ kg$^{-1}$ K$^{-1}$ for $Fe_3C$ (Ref 1). However, the steel must be processed in a very careful manner so as to yield very fine precipitates of titanium carbides. Usually, the carbon content of these steels lies between 0.06 and 0.08%. Therefore, a critical task is the suppression of the formation of pearlite.

Hot-rolled, high-strength sheet steels have been applied to cross and long members of suspension parts in automobiles (Ref 2) for weight reduction. A problem in press forming sheet steels having tensile strengths of 780 grade was lack of stretch flange formability (Ref 3). In general, stretch flange formability of high strength steel sheet can be improved by the increase in local ductility (Ref 4). From the view point of microstructure, ferritic steel without pearlite and large cementites have superior local ductility since it has less stress concentration regions (Ref 5) compared with multiphase microstructures such as dual phase and TRIP steels. Hence, stretch flange formability should be improved if microstructure of the steel can be controlled to be only ferrite without pearlite and large cementites.

Carbides precipitating just after austenite-ferrite transformation such as TiC easily (Ref 6) grow in hot-rolled low carbon steel because of high austenite-ferrite transformation temperature. Large precipitates of cementite at grain boundaries deteriorate stretch-flange formability (Ref 7, 8). Therefore, the size of the carbide precipitates can be refined by depressing the austenite-ferrite transformation temperature. One possible approach could be the addition of manganese.

This article reports the results of a study to achieve high strength (YS: 450 MPa min.) as well as adequate stretch flangeabilty in ~0.04-0.06% carbon steels through precipitation hardening by the precipitates of titanium carbide.

## 2. Experimental

### 2.1 Material

An experimental heat was produced in a vacuum induction furnace (vacuum level = 150 μm of Hg) with the addition of ferro-titanium with the target of 0.15 wt.% titanium in the steel. This melt was then poured into a 35 kg cylindrical ingot of 100 mm diameter. The ingot was subsequently soaked at 1175 °C for 2 h followed by hot rough rolling into 20 mm-thick plate.

### 2.2 Chemistry

The chemical composition of the steel was determined in the Optical Emission Spectroscope (OES). Nitrogen contents were determined in the Nitrogen Analyzer.

**B. Sarkar** and **B.K. Jha,** R&D Centre For Iron and Steel, Steel Authority of India Limited (SAIL), Ranchi, India. Contact e-mail: biswajitsarkar@rocketmail.com.

### 2.3 Thermo-Mechanical Processing

The dissolution temperature of titanium carbide precipitates was determined by the solubility product data (Ref 9): $\log_{10}[Ti][C] = -7000/T + 5.33$. The dissolution temperature of TiC precipitates was ~1135 °C for the steel in this study. The 20 mm plate was cut into three pieces. These were again soaked at 1175 °C and were hot rolled into 7 mm plates. These plates were further soaked at 1175 °C for half an hour and were hot rolled into 4 mm-thick plates at 1100, 1000, and 900 °C in single pass followed by air cooling.

### 2.4 Tests

The samples from the three plates rolled at the three temperatures of 1100, 1000, and 900 °C were prepared for optical microscopy. These were etched with 2% nital and observed in an optical microscope.

Fifty millimeter gauge length tensile samples were machined from the three thermo-mechanically processed plates. These were tensile tested at a cross head rate of 2 mm $min^{-1}$. in a tensile testing machine.

Transmission electron microscopy (TEM) studies were conducted on sample from plate that was rolled at 1000 °C. This plate had shown the highest yield strength of 484 MPa, UTS of 586 MPa, and elongation of 14.8%. Samples were mechanically thinned down to ~0.1 mm. These were jet polished in the twin jet polisher using an electrolyte consisting of perchloric acid and acetic acid. These thin foils were examined in the TEM operating at 200 kV.

### 2.5 Hole expansion test

Strips, 60 × 220 mm, were prepared from the 4 mm-thick hot-rolled plates. A 14 mm-diameter hole was drilled in each, and the strips were subjected to hole expansion test in the formability tester. Such testing involves forcing a punch through the holes until any one crack extends all through the test piece thickness. This extension of the crack was detected through a drop in the load at which point the punch descended automatically. The expanded holes were measured and were recorded. Hole expansion ratios were reported in % as follows:

$$\text{Hole expansion, } \lambda\,(\%) = (D_h - D_0) * 100/D_0$$

where $D_0$ = Original hole diameter ($D_0$ = 14 mm), $D_h$ = Hole diameter after rupture (mm).

## 3. Results and Discussion

Table 1 shows the chemical composition of the experimental steel along with $Ac_1$ and $Ac_3$ temperatures.

**Table 1 Chemical composition (wt.%), $Ac_1$ and $Ac_3$ temperatures**

| C | Mn | Si | Ti | S | P | Al | N, ppm | $Ac_1$, °C | $Ac_3$, °C |
|---|---|---|---|---|---|---|---|---|---|
| 0.04 | 0.81 | 0.38 | 0.15 | 0.01 | 0.013 | 0.043 | 39 | 725 | 948 |

The $Ac_1$ and $Ac_3$ temperatures were calculated using Andrew's (Ref 10) formula:

$$Ac_1 = 723 - 10.7 * Mn - 16.9 * Ni + 29.1 * Si + 16.9 * Cr + 290 * As + 6.38 * W$$

$$Ac_3 = 910 - 203 * SQRT(C) - 15.2 * Ni + 44.7 * Si + 104 * V + 31.5 * Mo + 13.1 * W - 30 * Mn - 11 * Cr - 20 * Cu + 700 * P + 400 * Al + 120 * As + 400 * Ti$$

Figures 1-3 display the optical micrographs of the samples from the plates that were rolled at 1100, 1000, and 900 °C in a single pass from 7 to ~4 mm. As evident from the microstructures, these steels are virtually pearlite free. The yield strengths of these plates were in the range of 434-484 MPa, the ultimate tensile strength varied from 508 to 586 MPa, while the elongation was in the range of 13-17.8% (see Table 2). Since the plate rolled at 1000 °C exhibited the greatest yield strength of 484 MPa, a detailed analysis of the sample from the plate was conducted. It showed a tensile

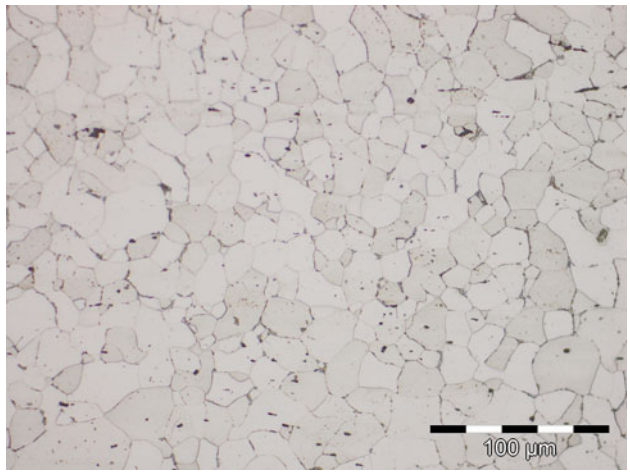


**Fig. 1** Optical micrograph of the sample from plate rolled at 1100 °C

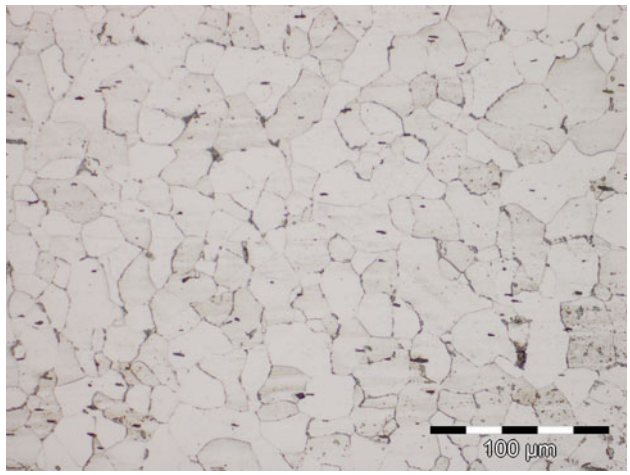


**Fig. 2** Optical micrograph of the sample from plate rolled at 1000 °C

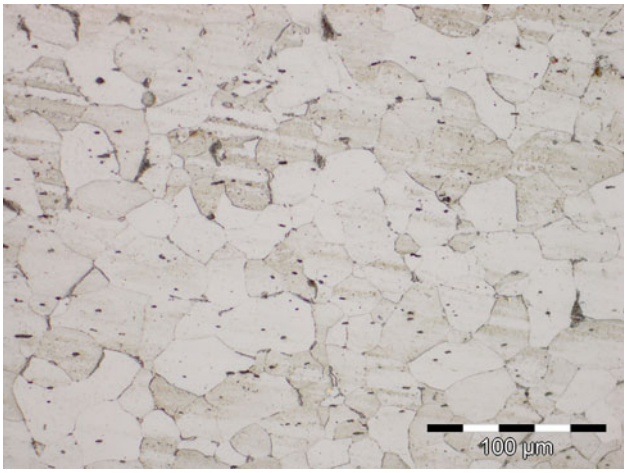


**Fig. 3** Optical micrograph of the sample from plate rolled at 900 °C

**Table 2 Tensile properties, hole expansion ratios, and ferrite grain size**

| Rolling Temp., °C | YS, MPa | UTS, MPa | % Elong., 50 mm GL | λ, % | Av. ferrite grain size, μm |
|---|---|---|---|---|---|
| 1100 | 462 | 578 | 13.0 | 26.0 | 24 |
| 1000 | 484 | 586 | 14.8 | 23.0 | 25 |
| 900 | 434 | 508 | 17.8 | 30.7 | 28 |

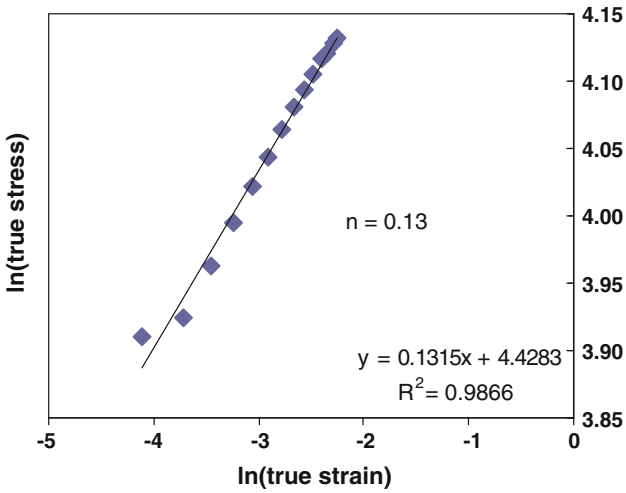


**Fig. 4** Plot of ln(true stress) vs. ln(true strain) for the sample with YS = 484 MPa

strength of 586 MPa. The total elongation was ~15%. Figure 4 is the ln(true stress) versus ln(true strain) plot for the steel. The strain hardening exponent ($n$) is 0.13 indicating adequate stretchability. Table 3 displays the reduction in area, true fracture stress, and hole expansion ratio for the samples from these plates. There appears to be a strong correlation between the true fracture stress and the hole expansion ratio (λ). A high λ is associated with a low true fracture stress (see Fig. 5). Figure 6 shows the bright field image TEM image of the precipitates at a magnification of 15,000×.

**Table 3 Reduction in area, true fracture stress, and hole expansion ratio**

| Rolling Temp., °C | Original area, $mm^2$ | Area at fracture ($A_f$), $mm^2$ | Reduction in area ($R_A$), % | True fracture stress (fracture load/$A_f$), MPa | λ, % |
|---|---|---|---|---|---|
| 1100 | 48.69 | 30.38 | 37.6 | 670.8 | 26.0 |
| 1000 | 47.78 | 28.9 | 39.5 | 693.2 | 23.0 |
| 900 | 50.74 | 29.02 | 42.8 | 652.8 | 30.7 |

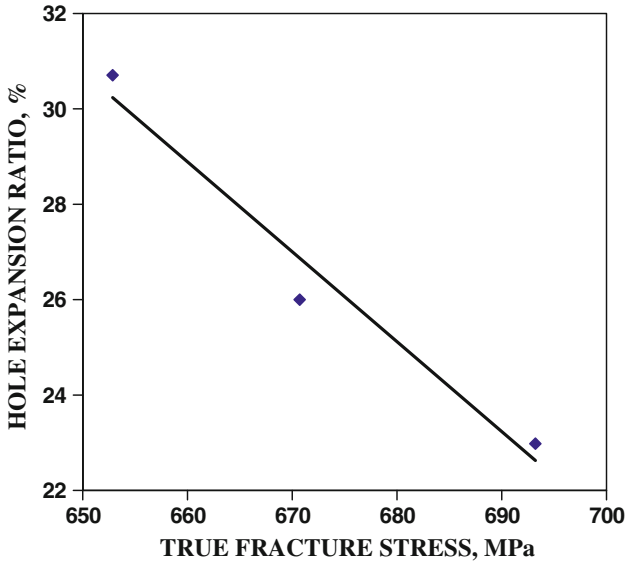


**Fig. 5** Plot of hole expansion ratio vs. true fracture stress

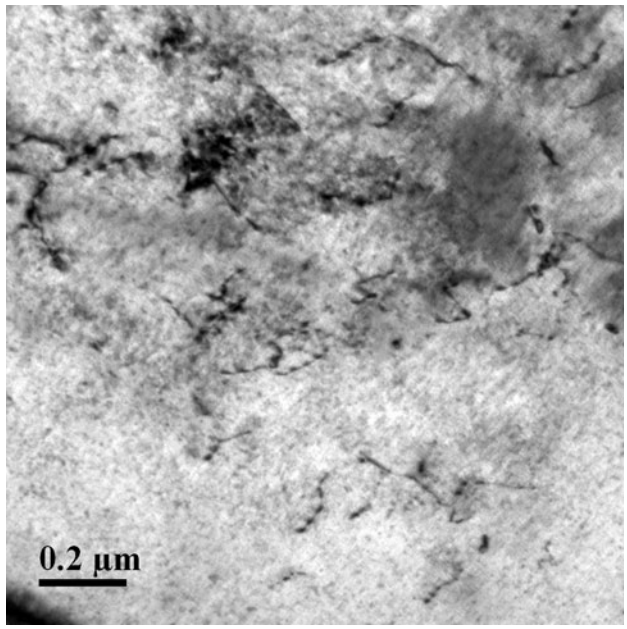


**Fig. 6** Bright field transmission electron microscope image showing titanium carbosulfide precipitates

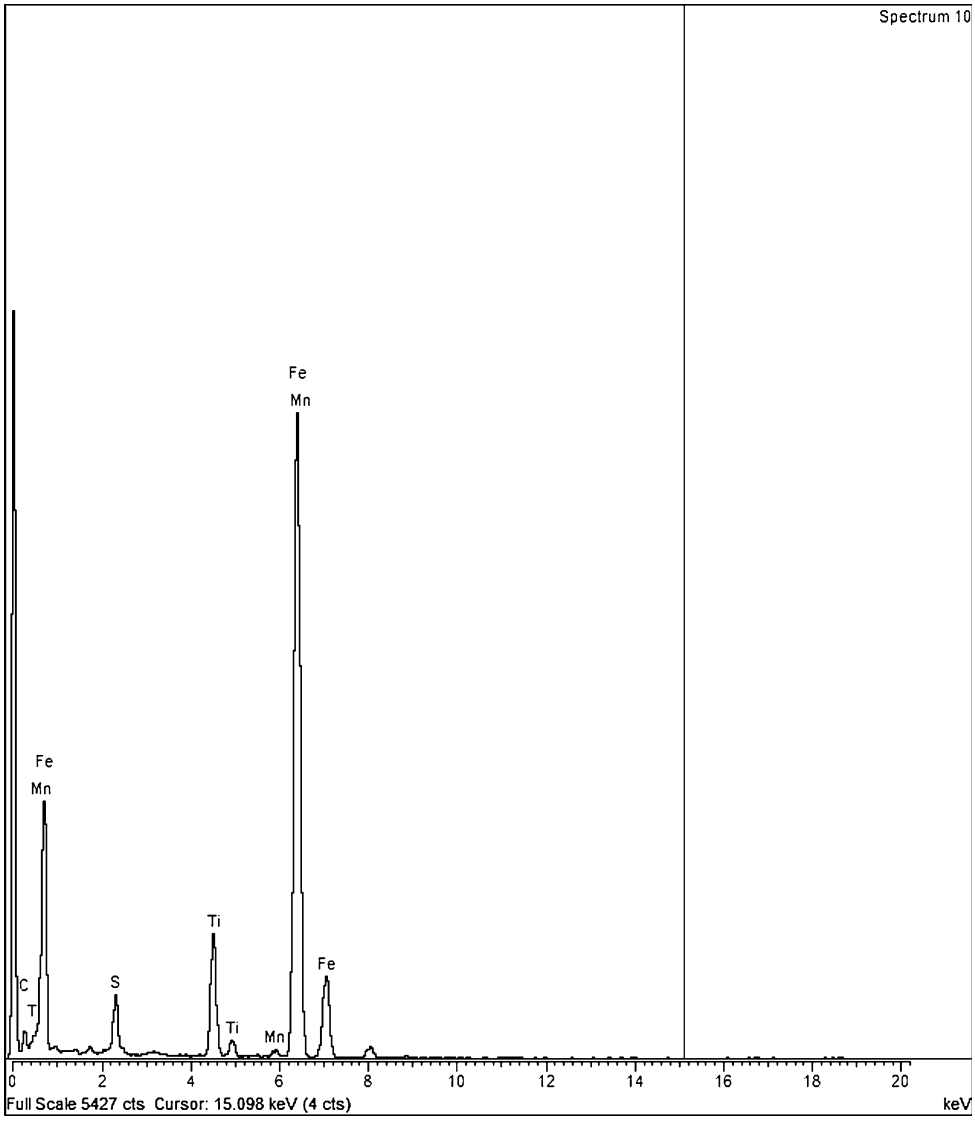


**Fig. 7** EDAX spectrum showing the precipitates to be of titanium carbosulfide

Figure 7 is the corresponding EDAX spectrum. It is observed that the precipitates are those of titanium carbosulfide.

Precipitates of titanium carbosulfides have been formed because of the relatively high (0.01 wt.%) sulfur content in the steel. Stretch flangeability of these plates was evaluated by carrying out hole expansion test The hole expansion ratios (λ) of these plates have been shown in Table 2. λ for these plates varied from 23 to 30.7%. The plate rolled at 1000 °C showed the highest yield strength (484 MPa) and a λ value of 23%. As mentioned earlier, λ values are a function of the homogeneity of the microstructure. Therefore, an extremely fine distribution of precipitates in ferrite facilitates the achievement of high λ values. In the present steel, precipitates size varied from ~300 to ~10 nm. Hence, for maximising λ, the larger precipitate sizes have to be refined further into smaller sizes.

The following strengthening mechanisms contribute toward the yield strength of steels (Ref 11):

$$\sigma = \sigma_0 + \Delta\sigma_s + \Delta\sigma_G + \Delta\sigma_d + \Delta\sigma_p$$

where σ = predicted yield strength, $\sigma_0$ = lattice friction stress (Ref 12), $\Delta\sigma_s$ = solid solution strengthening (Ref 13), $\Delta\sigma_G$ = Grain size hardening (Ref 14), $\Delta\sigma_d$ = Dislocation hardening, and $\Delta\sigma_p$ = Precipitation strengthening.

$$\sigma_0 = 48\,\text{MPa}$$

$$\begin{aligned}\sigma_s =& 4750[C] + 3750[N] + 37[Mn] + 84[Si]\\ =& 4750 * 0 + 3750 * 0 + 37 * 0.81 + 84 * 0.38\\ &\sim 62\,\text{MPa (Assuming negligible contribution from C and N in solid solution.)}\end{aligned}$$

$$\begin{aligned}\sigma_G =& k_y * d_F^{-1/2}, \quad k_y = 16.20\,\text{MPa mm}^{1/2},\\ d_F =& \text{Average grain size in mm}\\ =& 16.20 * (25 * 10^{-3})^{-1/2} \sim 102\,\text{MPa}\end{aligned}$$

Since the plates were hot rolled at 1000 °C and air cooled, the contribution from dislocation hardening ($\Delta\sigma_d$), can be ignored. Therefore, the contribution from precipitation strengthening ($\Delta\sigma_{p)}$ can be estimated as follows:

$$\Delta\sigma_p \sim 484 - (48 + 62 + 102) = 272\,\text{MPa}$$

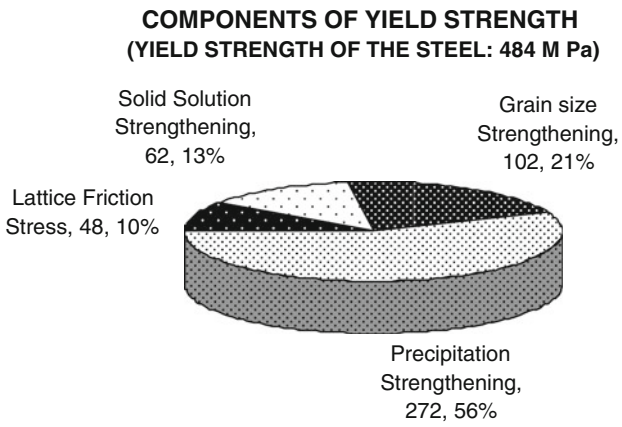


**Fig. 8** Pie chart showing the contributions from various strengthening mechanisms toward yield strength of 484 MPa achieved in the plate rolled at 1000 °C

Figure 8 is the pie chart showing the contributions from various strengthening mechanisms toward yield strength of 484 MPa. Therefore, it can be inferred that precipitation strengthening has been maximized in case of the plate rolled at 1000 °C. More than half of the yield strength is derived from precipitation strengthening (∼56%). The contribution from grain size to the yield strength is only ∼21% (see Fig. 8).

## 4. Conclusions

The following conclusions can be drawn from this study.

(i) The yield strength of the plates lay in the range of 434-484 MPa while the ultimate tensile strength varied from 508 to 586 MPa for the plates rolled from ∼7 to 4 mm in a single pass followed by air cooling. The % elongation varied from 13 to ∼18. The plate rolled at 1000 °C showed the highest yield and tensile strength of 484 and 586 MPa, respectively. The % elongation was ∼15.

(ii) The strain hardening exponent ($n$) is 0.13 indicating adequate stretchability.

(iii) Hole expansion ratio (λ) varied in the range from 23 to 30.7% for the plates rolled from ∼7 to ∼4 mm in single pass followed by air cooling. The plate rolled at 1000 °C showed a λ of ∼23%.

(iv) A strong negative correlation was found between the true fracture stress and hole expansion ratio (λ).

(v) Transmission Electron Microscopy revealed the presence of small precipitates (∼10-50 nm) of titanium carbosulfide.

## Acknowledgments

The authors' thanks are due to the management of the R & D Centre for Iron and Steel (RDCIS), the Steel Authority of India Ltd. (SAIL) for their permission to undertake this research. The help received from the respective staff of melting and solidification laboratories, the experimental rolling mill, metallography, and the mechanical and formability testing laboratories is gratefully acknowledged.

## References

1. F.D. Richardson, The Thermodynamics of Metallurgical Carbides and of Carbon in Iron, *J. Iron Steel Inst. Lond.*, 1953, **175**, p 33–51
2. S. Hashimoto, *J. JSAE*, 2000, **54**(1), p 39
3. K. Yamazaki and K. Koyama, *J. Jpn. Technol. Plast.*, 1994, **35**(404), p 1036
4. K. Matsudo, Y. Uchida, M. Yoshida, and K. Osawa, *J. Jpn. Technol. Plast.*, 1973, **14**(146), p 201
5. T. Inoue and S. Kinoshita, *J. Jpn. Technol. Plast.*, 1973, **14**(147), p 291
6. T. Shimizu, E. Yasuhara, O. Furukimi, and M. Morita, *CAMP-ISIJ*, 2000, **13**, p 411
7. N. Matsuzu, A. Itami, and K. Koyama, SAE Technical Paper Series No. 910513
8. T. Kashima and S. Hashimoto, *Tetsu-to-Hagane*, 2001, **87**(3), p 34
9. K.J. Irvine, F.B. Pickering, and T. Gladman, Grain Refined C-Mn Steels, *J. Iron Steel Inst.*, 1967, **205**, p 161
10. K.W. Andrew, *J. Iron Steel Inst.*, 1965, **203**(7), p 721
11. I. Kozasu, *Proceedings of Thermec "88*, ISIJ, Tokyo, 1988, p 420
12. R. Wang et al., Microstructure and Precipitation Behaviour of Nb, Ti Complex Microalloyed Steel Produced by Compact Strip Processing, *ISIJ Int.*, 2006, **46**(9), p 1345–1353
13. Q. Yong et al., *Microalloyed Steels—Physical and Mechanical Metallurgy*, The Mechanical Industry Press, Beijing, 1989, p 57
14. V. Thillou, *Basic Metal Processing Research Institute Report*, University of Pittsburgh, Pittsburgh, PA, USA, 1977